ACS APPLIED MATERIALS & INTERFACES

Research Article

www.acsami.org

Pressure-Induced Changes in Interdiffusivity and Compressive Stress in Chemically Strengthened Glass

Mouritz N. Svenson,[†] Lynn M. Thirion,[‡] Randall E. Youngman,[‡] John C. Mauro,[‡] Sylwester J. Rzoska,[§,∥] Michal Bockowski,[§] and Morten M. Smedskjaer*[,†]

[†]Section of Chemistry, Aalborg University, Aalborg 9000, Denmark

[‡]Science and Technology Division, Corning Incorporated, Corning, New York 14831, United States

[§]Institute of High Pressure Physics, Polish Academy of Sciences, Warsaw 00-142, Poland

[∥]Institute of Physics, University of Silesia, Chorzow 41-500, Poland

Supporting Information

ABSTRACT: Glass exhibits a significant change in properties when subjected to high pressure because the short- and intermediate-range atomic structures of glass are tunable through compression. Understanding the link between the atomic structure and macroscopic properties of glass under high pressure is an important scientific problem because the glass structures obtained via quenching from elevated pressure may give rise to properties unattainable under standard ambient pressure conditions. In particular, the chemical strengthening of glass through K^+-for-Na^+ ion exchange is currently receiving significant interest due to the increasing demand for stronger and more damage-resistant glass. However, the interplay among isostatic compression, pressure-induced changes in alkali diffusivity, compressive stress generated through ion exchange, and the resulting mechanical properties are poorly understood. In this work, we employ a specially designed gas pressure chamber to compress bulk glass samples isostatically up to 1 GPa at elevated temperature before or after the ion exchange treatment of a commercial sodium−magnesium aluminosilicate glass. Compression of the samples prior to ion exchange leads to a decreased Na^+−K^+ interdiffusivity, increased compressive stress, and slightly increased hardness. Compression after the ion exchange treatment changes the shape of the potassium−sodium diffusion profiles and significantly increases glass hardness. We discuss these results in terms of the underlying structural changes in network-modifier environments and overall network densification.

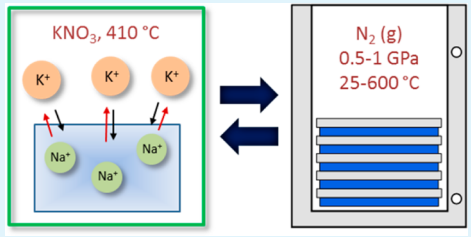

KEYWORDS: *ion exchange, compression, glass, NMR, hardness, chemical strengthening*

INTRODUCTION

The application of pressure enables precise tuning of the interatomic distances and bonding patterns in a material. In crystalline solids, compression can lead to phase transformations, producing structures with unusual chemical and physical properties.[1] A classic example is the pressure-induced transformation of soft graphite with sp^2 C−C bonding into hard diamond with sp^3 C−C bonding.[2] More recently, advances in experimental and theoretical techniques at high pressure have enabled the synthesis of new superconductors[3,4] and the discovery of metal-to-semiconductor transitions.[5] For crystalline materials, compression has thus become an important tool in the synthesis of new materials via phase transformations.[1,6,7] However, comparable breakthroughs in attainment of unique properties for glassy materials through compression on an industrial scale are still lacking.

When a glassy material is subjected to sufficiently high pressure, significant changes can take place in the short- and intermediate-range structures and thereby alter the macroscopic physical properties.[8−10] Although these structural changes under high pressure are still not well understood, topological changes facilitating densification have been found to include changes in the coordination number of network-former ions,[11] volumetric compaction of network-modifier sites,[11] and changes in intermediate-range atomic order.[11,12] Permanent densification of glass is conventionally achieved by cold compression in diamond anvil cells at pressures above 8−10 GPa.[13] This method allows experiments to be performed in the high-pressure regime and has led to interesting results on pressure-induced structural changes in glass.[12] However, only small sample specimens can be processed,[14] and subsequent characterization of macroscopic properties (e.g., mechanical properties) is often impossible. By performing compression experiments at elevated temperature, permanent densification is obtainable at much lower pressures,[15,16] enabling processing of larger sized specimens. If novel glass properties can be obtained through such experiments, this approach has the potential to be industrially relevant. Mild compression at elevated temperature has been shown to affect a range of properties of glasses including hardness,[17] optical properties,[16] and elastic mod-

Received: April 2, 2014
Accepted: June 9, 2014
Published: June 9, 2014

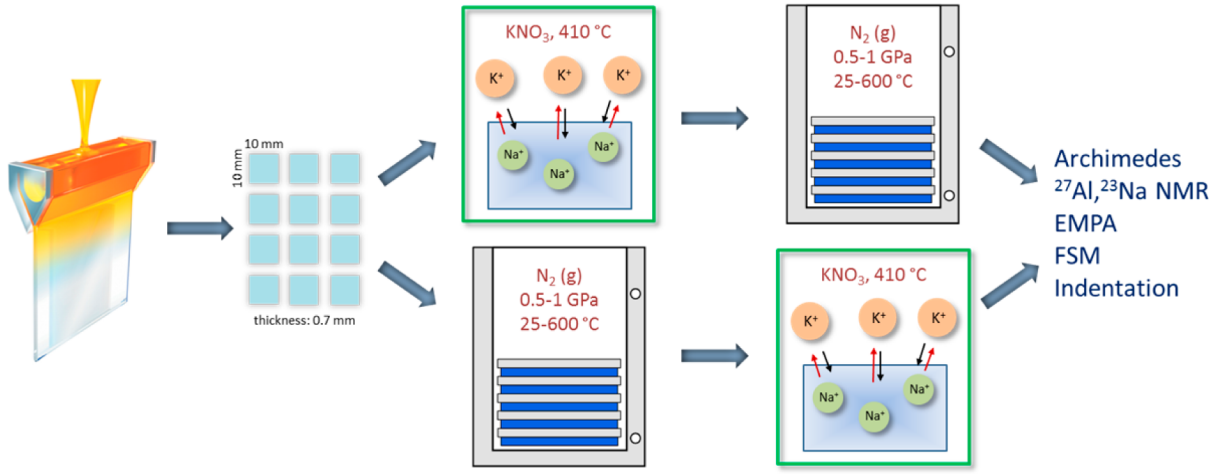

Figure 1. Schematic illustration of the experimental approach. Fusion-drawn glass sheets are cut to the dimensions of 10 × 10 × 0.7 mm^3. These glass samples are then subjected to ion exchange treatment in a KNO_3 bath either before or after a hot isostatic compression at 0.5 or 1 GPa and are referred to as postcompressed (upper part) or precompressed (lower part) samples, respectively. Following compression and ion exchange, density is measured using Archimedes' principle, structure is characterized through ^{27}Al and ^{23}Na NMR, potassium diffusion profiles are determined using EMPA, depth of layer and compressive stress are determined by optical FSM measurements, and hardness is determined by Vickers indentation.

uli,[18,19] as well as short-range network structure.[16] In this study, isostatic compression experiments are performed using a specially designed gas pressure chamber with large inner volume (up to 100 mm), enabling simultaneous application of high pressure (up to 1 GPa) and high temperature (>1000 °C).

Improvements in strength and damage resistance have proven to be vital attributes for enabling new advanced applications of glass.[20−22] Various methods of glass strengthening (e.g., thermal tempering, ion exchange, and surface crystallization) are utilized for commercial glasses.[23] Chemical strengthening through ion exchange has the capability of introducing high compressive stress in thin plates without optical distortion, leaving it as the leading candidate for strengthening of cover glasses. This chemical strengthening is achieved by the exchange of a small alkali ion (Na^+) with a larger one (K^+) in the glass surface by interdiffusion upon submersion in a liquid salt bath (KNO_3). This results in the formation of a compressive stress at the surface and enhancement of the strength and damage resistance of the glass. However, the effective increase of damage resistance achievable by this method is limited by compositional and topological restrictions pertaining to the given glass.[23,24] In addition, understanding the basics of the alkali interdiffusion is of critical importance for optimization of this strengthening approach.

In this work, we investigate the ion exchange characteristics (magnitude and depth of the compressive stress layer) of samples subjected to isostatic compression before or after the ion exchange treatment. The experiments are performed on a commercial sodium−magnesium aluminosilicate glass.[25] This provides information on the pressure-induced changes in alkali diffusivity, the relationship between isostatic compression and generated compressive stress, and its effect on the mechanical properties of the glass, which we quantify here through Vickers indentation. To link the trends in ion exchange characteristics and hardness to the local atomic network structures, we have also performed nuclear magnetic resonance (NMR) measurements at high field on selected samples. The experimental approach is illustrated in Figure 1. With this study, we thus shed light on the possibility of combining isostatic compression with ion exchange to generate novel glass properties.

EXPERIMENTAL SECTION

Sample Preparation. The glass under investigation is a commercial sodium−magnesium aluminosilicate composition with glass transition temperature T_g = 652 °C.[25] Fusion-drawn glass sheets with dimensions of approximately 10 × 10 × 0.7 mm^3 were used. The glass samples were subjected to ion exchange treatment either before or after an isostatic compression at 0.5 or 1 GPa. In the following, samples compressed after ion exchange are referred to as *postcompressed*, while samples compressed prior to ion exchange are referred to as *precompressed*. In addition, a base glass subjected only to ion exchange treatment was also prepared.

The ion exchange treatment was performed in a molten KNO_3 salt bath by submersion for 10 h at 410 °C. This effectively exchanged K^+ from the salt bath for Na^+ in the glass surface, with only minor changes in the amount of other elements or total alkali concentrations.[26] The isostatic compression was performed by loading individual samples into a vertically positioned gas pressure chamber with an internal diameter of 6 cm. A multizone cylindrical graphite furnace was placed inside the gas pressure reactor with nitrogen as the compression medium. To monitor the temperature during the experiments, PtRh6%−PtRh30% thermocouples were used. The pressure was measured by Manganin gauges positioned in the low temperature zone of the reactor. The pressure and temperature were stabilized with an accuracy of 1 MPa and 0.1 K, respectively. The samples were heated with a constant rate of 600 K/h to the desired temperature (room temperature, 450 °C, or 600 °C). The system was kept at these conditions under high nitrogen pressure (0.5 or 1 GPa) for 1 h. Afterward, the furnace was cooled to room temperature at a constant rate of 60 K/min, and the system was decompressed at a rate of 30 MPa/min at room temperature.

Characterization. All of the samples were subjected to four types of analyses to determine density, hardness, compositional depth profiles of potassium, surface compressive stress, and the depth of the compressive stress layer. In addition, ^{23}Na and ^{27}Al NMR measurements were performed on two of the precompressed glasses and the glass sample that was only subjected to ion exchange (i.e., without pressurization). Density (ρ) was determined using Archimedes' principle with water as the immersion medium. Each measurement of sample weight was repeated at least 10 times. The Vickers hardness (H_V) of the samples was determined using a microindenter (Duramin 5, Struers A/S). A minimum of 60 indents were conducted on each

sample using an indentation time of 10 s and an indentation load of 9.81 N. The measurements were performed in air at room temperature.

To study the effects of pre- and postcompression on the K^+-for-Na^+ diffusion process, compositional depth profiles of potassium were determined using an electron micro probe analyzer (EMPA). The measurements were performed on a JEOL 8900R Superprobe (JEOL USA, Inc., Peabody, MA) equipped with 5 WDS spectrometers. The penetration depth of the potassium ions due to ion exchange was also measured using an FSM-6000 instrument (Orihara Industrial Co., Ltd.), which also provides the surface compressive stress. The K^+-for-Na^+ ion exchange gives the glass surface a higher refractive index than the interior, that is, the surface can act as a waveguide. This is utilized in the FSM instrument to record optical fringe patterns, giving an upper set of fringes corresponding to the TM mode of light propagation and a lower set of fringes corresponding to the TE mode. The offset in position between the first TM and TE fringes gives the birefringence, which, when multiplied by the stress-optic coefficient, yields the surface compressive stress (CS) of the glass. The depth of the compressive layer (DOL) is calculated from the number of fringes and the width of the fringe pattern based on the TM mode data. A total of eight FSM measurements were performed on each sample. Examples of the optical FSM fringe patterns are shown in Figure S1 (Supporting Information).

^{27}Al and ^{23}Na magic-angle spinning (MAS) and multiple quantum MAS (MQMAS) NMR experiments were conducted at 16.4 T, using a commercial spectrometer (Agilent) and 3.2 mm MAS NMR probe. The resonance frequencies at this external magnetic field were 182.34 and 185.12 MHz for ^{27}Al and ^{23}Na, respectively. Samples were crushed and loaded into 3.2 mm zirconia rotors, which gave a small ^{27}Al background signal that was identified by running duplicate MAS NMR experiments on the empty rotors. Sample spinning was controlled to 20 ± 0.01 kHz. MAS data for both nuclei were collected using short radio frequency pulses of 0.6 μs (π/12 tip angle), 2−5 s recycle delays, and signal averaging of 1000 scans. Data were processed without apodization and shift referenced to aqueous $Al(NO_3)_3$ and aqueous NaCl, both at 0.0 ppm. ^{27}Al MAS NMR spectra were fit with DMfit and the Czjzek model to account for distributions in quadrupolar coupling parameters.[27]

MQMAS NMR spectra were collected for ^{27}Al (^{23}Na) using the three pulse, zero quantum filtering method.[28] The hard $\pi/2$ and $3\pi/2$ pulse widths were calibrated to 1.1 (1.6) and 3.3 (4.8) μs, and the soft reading pulse of the z-filter was optimized to 15 (20) μs. In the case of ^{27}Al, 24 scans were collected for each of 200 t_1 points, using a recycle delay of 0.5 s. For ^{23}Na, 48 scans with a 2 s recycle delay were used to collect 40 t_1 points. Spectra were processed using commercial software (VNMRJ, Agilent) and modest line broadening (200 and 100 Hz for ^{27}Al, ^{23}Na). For each resonance in the 3QMAS NMR spectra, the centers of gravity in the MAS and isotropic dimensions, δ_2^{CG} and δ_{iso}^{CG}, are used to calculate the isotropic chemical shift (δ_{CS}) and the quadrupolar coupling product (P_q) according to

$$\delta_{CS} = \frac{10}{27}\delta_2^{CG} + \frac{17}{27}\delta_{iso}^{CG} \quad (1)$$

and

$$P_q = (\delta_{iso}^{CG} - \delta_2^{CG})^{1/2} f(S)\, \nu_0 \times 10^{-3} \quad (2)$$

where $f(S)$ = 10.244 for spin-5/2 nuclei (^{27}Al) or 5.122 for spin-3/2 nuclei (^{23}Na), and ν_0 is the resonance frequency of the quadrupolar nucleus in megahertz (MHz).[28] P_q from eq 2 can be related to the quadrupolar coupling constant (C_q) as $P_q = C_q(1 + \eta_q^2/3)^{1/2}$, where η_q is the quadrupolar coupling asymmetry parameter. P_q and C_q are often used interchangeably, with small errors introduced by ignoring the contribution of η_q.

RESULTS

Network Densification. The densities of both the precompressed (i.e., compressed prior to ion exchange) and postcompressed (i.e., compressed after ion exchange) samples are plotted as a function of the compression temperature in Figure 2. The densities of the base glass with and without ion exchange treatment are also shown. In addition, density and other results are summarized in Tables 1 and 2. Both sample series exhibit a similar increase of density as compression pressure and temperature increase, comparable with literature results for similar conditions.[16] There are no significant differences in the densities of the pre- and postcompressed samples for the same pressurization conditions (i.e., pressure and temperature). In addition, the ion exchange treatment of the base glass does not significantly affect its density.

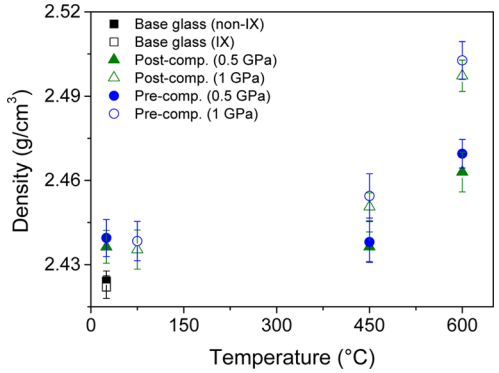

Figure 2. Density as a function of compression temperature of samples compressed at 0.5 or 1 GPa before or after ion exchange. The densities of the noncompressed base glasses with or without ion exchange (IX) are also shown.

Table 1. Density (ρ), Vickers Hardness (H_V), Surface Compressive Stress (CS), and Depth of Layer (DOL) of the Base Glass with and without Ion Exchange (IX)

	non-IX	IX
ρ (g/cm^3)	2.424 ± 0.004	2.422 ± 0.004
H_V (GPa)	5.9 ± 0.3	8.4 ± 0.4
CS (MPa)[a]	NA	946 ± 2
DOL (μm)[a]	NA	48.9 ± 0.1

[a]Values of CS and DOL are from the optical FSM measurements.

Interdiffusivity and Compressive Stress. The compositional depth profiles of K_2O of the pre- and postcompressed samples are shown in Figure 3. Potassium is incorporated into the glass surface due to the K^+-for-Na^+ interdiffusion process, and the concentration profiles of sodium ions thus decrease proportionally to the increase in concentration of potassium ions. The surface concentrations of other elements in the glass exhibit only minor variations with depth (not shown).

Compression of the glass around room temperature prior to ion exchange does not change the Na−K interdiffusivity (Figure 3a). However, as the compression temperature and pressure are increased and the structure densifies (Figure 2), the diffusion depth decreases (Figure 3a). The potassium depth profiles of ion exchanged glasses typically follow a complementary error function.[29] Indeed the ion-exchanged base glass and the precompressed glasses can be fitted relatively well with this function (Figure S2, Supporting Information). These trends in DOL with compression conditions based on the EMPA measurements are supported by the optical FSM measurements. In addition, the latter data show how CS varies

Table 2. Density (ρ), Vickers Hardness (H_V), Surface Compressive Stress (CS), and Depth of Layer (DOL) of the Glasses Subjected to Isostatic Compression before or after Ion Exchange Treatment

condition		ρ (g/cm^3)		H_V (GPa)		CS (MPa)[a]		DOL (μm)[a]	
P (Gpa)	T (°C)	postcomp.	precomp.	postcomp.	precomp.	postcomp.	precomp.	postcomp.	precomp.
0.5	25	2.436 ± 0.006	2.440 ± 0.007	8.3 ± 0.3	6.3 ± 0.2	933 ± 2	929 ± 4	49.6 ± 0.6	50.8 ± 0.2
0.95	75	2.435 ± 0.007	2.438 ± 0.007	8.2 ± 0.3	6.4 ± 0.2	923 ± 3	930 ± 4	48.9 ± 0.3	50.2 ± 0.7
0.5	450	2.436 ± 0.005	2.438 ± 0.007	8.0 ± 0.2	6.4 ± 0.2	577 ± 3	939 ± 13	58.8 ± 0.1	45.1 ± 0.6
1	450	2.450 ± 0.005	2.454 ± 0.008	7.6 ± 0.3	6.1 ± 0.3	569 ± 4	939 ± 8	54.9 ± 0.9	38.8 ± 0.1
0.5	600	2.463 ± 0.007	2.470 ± 0.005	6.8 ± 0.3	7.0 ± 0.3	NA	1104 ± 19	NA	18.8 ± 0.2
1	600	2.497 ± 0.006	2.503 ± 0.007	6.9 ± 0.3	6.7 ± 0.3	NA	1240 ± 10	NA	9.8 ± 0.4

[a]Values of CS and DOL are from the optical FSM measurements.

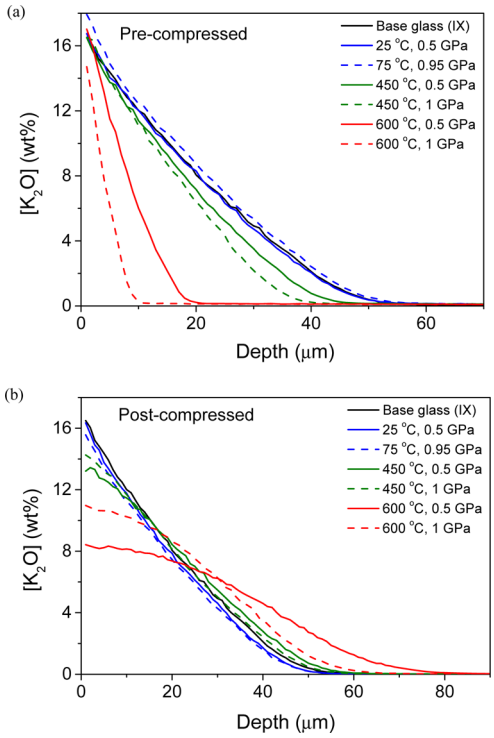

Figure 3. K_2O concentration profiles of the samples that have (a) first been isostatically compressed at different temperatures and pressures (see labels) and then ion exchanged or (b) first been ion exchanged and then isostatically compressed at different temperatures and pressures (see labels). The K_2O concentration profile of the base glass only subjected to ion exchange is also shown.

with compression conditions. These values of DOL and CS are reported in Table 2. Isostatically compressing the samples before ion exchange causes an increase of CS for samples pressurized at 600 °C.

Postcompression of the samples following ion exchange at 410 °C causes distinct changes in the potassium diffusion profiles (Figure 3b). The peak concentration of K_2O at the surface decreases with increasing compression temperature or with decreasing pressure. On the other hand, DOL increases with increasing compression temperature or with decreasing pressure. Furthermore, postcompression leads to a decrease of CS compared to that of the noncompressed samples (Table 2). Again, this effect is more pronounced for compression at high temperature and low pressure. Figure 4 shows the correlation between the compressive surface stress and the depth of layer for both series of samples compressed at different conditions. The compressive surface stress generally decreases with increasing DOL, and thus, it is difficult to obtain samples

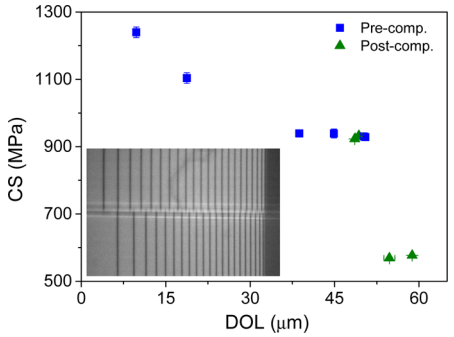

Figure 4. Dependence of compressive stress (CS) at the surface due to ion exchange on the potassium depth of layer (DOL) in the pre- and postcompressed samples (Table 2). (Inset) Example of optical fringe pattern from FSM used to determine CS and DOL in the ion exchanged glasses. The upper set of fringes in the image corresponds to the TM mode of light propagation, while the lower set of fringes corresponds to the TE mode.

through this approach with simultaneously high values of CS and DOL.

Glass Hardness. The dependence of Vickers hardness on compression temperature for both sample series is shown in Figure 5, in addition to the results of the base glass. Ion exchange of the base glass leads to a pronounced increase in hardness (from 5.9 to 8.4 GPa). Precompression of the samples results in only a small increase in hardness. This increase in hardness is greater for samples compressed at 600 °C. When the samples are subjected to postcompression, the hardness

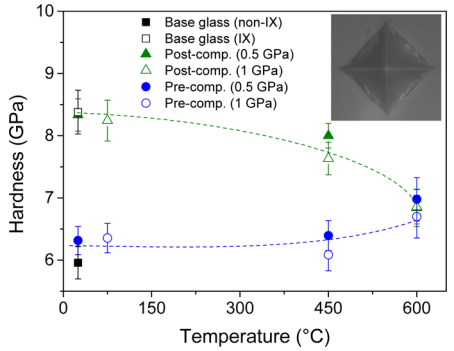

Figure 5. Vickers hardness as a function of compression temperature of samples compressed at 0.5 or 1 GPa before or after ion exchange. The hardness of the noncompressed base glasses with or without ion exchange are also shown. The dashed lines serve as guides for the eye. (Inset) Example of optical micrograph of indent produced by Vickers indentation and used to determine hardness.

dx.doi.org/10.1021/am5019868 | ACS Appl. Mater. Interfaces 2014, 6, 10436−10444

increase caused by ion exchange is gradually "reversed" as the compression temperature increases. These different trends in hardness indicate that different structural mechanisms govern the hardness variations between the two sample series.

Short-Range Glass Structure. ^{27}Al and ^{23}Na NMR measurements have been performed on the glass only subjected to ion exchange and the two precompressed glasses subjected to the highest (1 GPa at 600 °C) and lowest (0.5 GPa at 25 °C) temperature and pressure. Figure 6 shows the ^{27}Al MAS

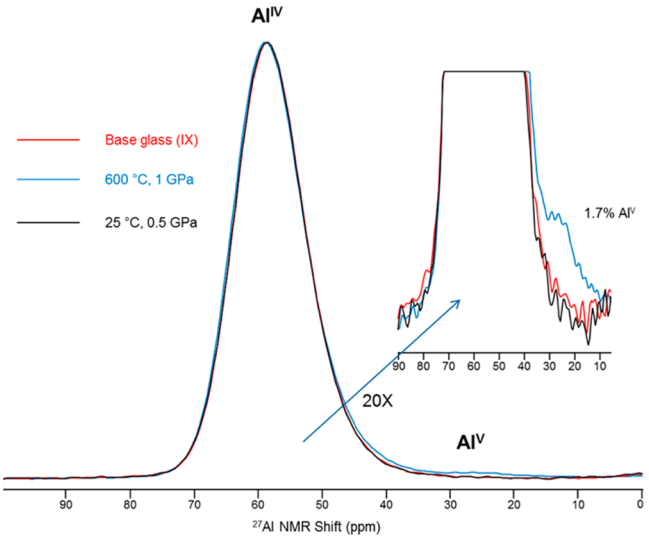

Figure 6. ^{27}Al MAS NMR spectra at 16.4 T of the base glass only subjected to ion exchange and two of the precompressed glasses (0.5 GPa at 25 °C and 1 GPa at 600 °C). Resonances due to 4-fold coordinated aluminum (Al^{IV}) and 5-fold coordinated aluminum (Al^{V}) are indicated.

NMR spectra at 16.4 T of these three samples. The peak at around +60 ppm, found in all three samples, is due to aluminum in tetrahedral coordination (Al^{IV})[30]. This is in agreement with the base glass being peralkaline, and there is thus sufficient concentration of charge-balancing modifier cations to stabilize all aluminum in tetrahedral configuration. However, for the glass precompressed at 1 GPa at 600 °C, the peak is asymmetrically broader on the more shielded side (lower shift), due in part to second-order quadrupolar effects and the presence of an additional ^{27}Al resonance near 30 ppm, assigned to 5-fold coordinated aluminum (Al^{V}). As shown in Figure S3 (Supporting Information), further evidence for the presence of Al^{V} groups has been obtained from ^{27}Al 3QMAS NMR analysis of this glass. Using DMFit[27] to simulate the ^{27}Al MAS NMR lineshapes in this glass, the fraction of Al^{V} is found to be approximately 1.7% (Figure S4, Supporting Information). Hence, the isostatic compression forces some aluminum species into 5-fold coordination even though the glass is peralkaline and this change is (partially) stable during the subsequent ion exchange at 410 °C. This is consistent with higher coordinated Si at high pressure[31] and changes in Al speciation in aluminosilicate glasses at even higher pressures.[11]

^{23}Na MAS NMR spectra at 16.4 T of the same three samples are shown in Figure 7. Although these glasses were all subjected to K^+-for-Na^+ exchange, the majority of the bulk material is unaffected, and thus, ^{23}Na NMR could be performed to examine impact of both pressure (compression) and temperature (annealing in the salt batch). There is a small increase in

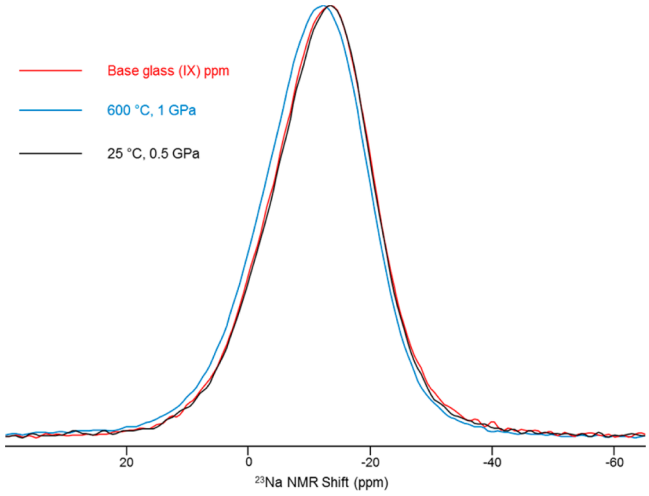

Figure 7. ^{23}Na MAS NMR spectra at 16.4 T of the base glass only subjected to ion exchange and two of the precompressed glasses (0.5 GPa at 25 °C and 1 GPa at 600 °C).

frequency of the glass precompressed at 1 GPa at 600 °C compared to the base glass, which is due to a decrease in the mean Na−O bond length.[16] This change is of smaller magnitude than that indicated in previous reports,[16,32−34] but this could be due to relaxation during the subsequent annealing (ion exchange) and the use of relatively modest pressures compared with the literature results. There appears to be a minor decrease in the shift of the glass precompressed at 0.5 GPa at room temperature, indicating a slightly increased Na−O bond length, especially when compared with that of the sample precompressed at 1 GPa at 600 °C. Differences between the lower compression and ion-exchanged-only glasses are similar to changes in sodium silicate glasses,[35] where Na^+ is surrounded by a combination of bridging and nonbridging oxygen.

To further study the sodium speciation, ^{23}Na 3QMAS NMR data have also been collected (Figure S5a, Supporting Information). On the basis of peak positions in the MAS and isotropic dimensions, these data show significant changes in P_Q and δ_{CS} for ^{23}Na (Figure S5b, Supporting Information). The results are summarized in Table 3 and are entirely consistent

Table 3. Quadrupolar Coupling Constant (P_Q) and Isotropic Chemical Shifts (δ_{CS}) Estimated from ^{23}Na 3Q MAS NMR Data of the Base Glass Only Subjected to Ion Exchange and Two of the Precompressed Glasses (0.5 GPa at 25 °C and 1 GPa at 600 °C)[a]

	δ_{CS} (ppm)	P_Q (MHz)
base glass (IX)	−8.5	2.24
0.5 GPa at 25 °C	−8.9	2.06
1 GPa at 600 °C	−8.1	1.87

[a]On the basis of measurement errors of isotropic and MAS NMR shifts, the errors of δ_{CS} and P_Q are estimated to be ±0.2 ppm and ±0.2 MHz, respectively.

with ^{23}Na NMR studies of Na^+ in aluminosilicate glasses.[36] The changes in δ_{CS} primarily reflect changes in Na−O bond length and are found to be in agreement with the ^{23}Na MAS NMR data, where a definite shortening of the average Na−O bond length was observed in the precompressed glass at 1 GPa and 600 °C. The changes in P_Q are also significant and account for at least part of the shifts in the MAS peak positions. P_Q is

sensitive to symmetry around the Na^+ site, which is thus affected by the ion exchange and isostatic compression both at room temperature and 600 °C and indicates a more symmetric bonding environment for Na^+ in the precompressed glasses. Previous studies of sodium in compressed oxide glasses typically focused on changes in ^{23}Na MAS NMR peak position, drawing on the correlation between chemical shift and average Na−O bond length.[36−40] However, as these results show, the change in P_Q with compression is not insignificant and further demonstrates the sensitivity of modifier environment to compression.

DISCUSSION

CS and DOL of Precompressed Glasses. Densification of the samples exhibits a strong dependence on both the temperature and pressure used for compression (Figure 2). For both the precompressed and postcompressed series, an inverse correlation of CS with DOL is observed (Figure 4). For the precompressed series, the decrease in DOL follows an increasing densification, showing a clear connection between network compaction and steric hindrance for Na−K interdiffusion. That is, glasses with densified structures have little available space and hence large activation barriers for interdiffusion. This is because these modifier cations move through the interstitial space in the network. A decrease of alkali diffusivity with network compaction, caused by annealing at ambient pressure, has also been previously reported.[41] The highest compressive stresses were obtained in the samples precompressed at 600 °C, that is, in the glasses with the lowest DOL and lowest amounts of incorporated K_2O. Hence, there must be a larger amount of stress generated for each K^+ ion stuffed into these samples. This indicates that the linear network dilation coefficient (B) increases as a result of pressurization for these conditions. Here, B is defined as the linear strain of the glass per unit change in alkali concentration. The relation between CS and B is seen by considering the expression for generated stress obtained via the ion exchange process (neglecting stress relaxation),

$$\sigma(z) = -\frac{BE}{1-\nu}[C(z) - C_{avg}] \quad (3)$$

where E is Young's modulus, ν is Poisson's ratio, and $C(z)$ and C_{avg} are the local concentration of K^+ at a penetration depth z in the glass and average concentration of K^+ throughout the glass, respectively. While the effect of pressurization at 1 GPa on Poisson's ratio should be small, an increase of Young's modulus of less than ∼10% is expected on the basis of previous findings.[17] However, such change in E cannot alone explain the significant increase in CS observed for the samples precompressed at 600 °C (Table 2). For these samples, there is thus a larger strain per unit of ions exchanged after pressurization (larger B value), presumably due to the decreased Na−O bond length, as confirmed by the NMR measurements on the sample precompressed at 1 GPa and 600 °C (Figure 7).

CS and DOL of Postcompressed Glasses. Postcompression of the samples increases DOL but decreases CS. This is likely a result of the thermal annealing during the isostatic compression, which causes inward diffusion of the potassium ions (i.e., increasing DOL) due to the concentration gradient across the sample. Because the surface concentration of potassium is consequently decreased (Figure 3b), the compressive stress at the surface also decreases according to eq 3. Hence, the generated compressive stress due to ion exchange can be relaxed at elevated temperature, even under an applied pressure of 1 GPa.

Effects of Densification and Compressive Stress on Glass Hardness. Hardness is governed by the surface properties of the glass into which the indenter penetrates. Ion exchange of the base glass causes an increase of hardness (Table 1). Figure 8 shows that for the postcompressed glass

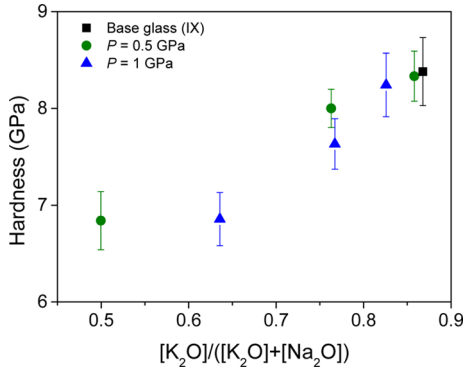

Figure 8. Dependence of Vickers hardness on the relative $[K_2O]/([Na_2O] + [K_2O])$ surface content for the samples that have first been ion exchanged and then isostatically compressed at different temperatures and pressures (postcompressed series). The K_2O and Na_2O concentrations are measured at a depth of ∼1 μm. The data of the noncompressed base glass only subjected to ion exchange is also shown.

series, hardness increases as a function of the amount of K_2O in the outermost surface layer, even though all hardness values are lower than that of the ion exchanged base glass. Two approximately linear trends appear in this plot for samples pressurized at 0.5 and 1.0 GPa, respectively, indicating the existence of a pressure-dependent mechanism for the hardness change.

For the precompressed glass series, the combined compression and ion exchange treatment did not effectively increase the hardness (Figure 5). To understand the structural origin of this behavior, a comparison between the samples post- and precompressed at 25 °C and at 0.5 GPa is used as the basis for the following discussion. These samples possess nearly identical values of all measured properties (i.e., K_2O concentration profile, depth of layer, compressive stress, and density), except hardness. Because the hardness variations of the postcompressed samples appear to be primarily a function of the K_2O concentration in the surface layer (Figure 8), it suggests that precompression causes a change in the properties of this K_2O-rich surface layer. Structural changes caused by pressurization cause the precompressed glasses to be in another (densified) state during the ion exchange process than those subjected to postcompression. Therefore, a discussion of the structural changes expected from room temperature compression at 0.5 GPa is given in the following.

Structural Changes upon Compression. Prior to compression, Si^{4+} is exclusively tetrahedrally coordinated. This is also the case for Al^{3+}, charge-compensated by Na^+ (Figure 6). The structural role of Mg^{2+} is not well understood,[42] with studies suggesting tetrahedral[43] and octahedral[42−44] coordination in highly distorted environments.[42] It has been suggested that Mg^{2+} coordination is affected by the field strength of the competing modifier ions, with low fields strength cations (e.g., Na^+ and K^+) favoring

tetrahedral Mg^{2+} coordination,[42,43] that is, tetrahedral Mg^{2+} is expected to be present in the glass under investigation. Partial competition of Mg^{2+} with silicon and aluminum for positions in the glass network has also been suggested.[45] During compression at relatively low pressure and temperature (0.5 GPa and 25 °C), an elastic densification of the glass is expected,[46] primarily resulting from changes in bond angles between the silica network tetrahedra.[47−49] This is not expected to affect the aluminum environments significantly, because aluminum species are expected to be present in rings of smaller angles,[50] not disposed to reconfigurations within this pressure regime.[51] Also, no permanent changes in the coordination numbers of Si^{4+}[52] or Al^{3+}[47,52] are expected. This is confirmed for Al^{3+} by the ^{27}Al MAS NMR results of the precompressed sample at 0.5 GPa and 25 °C (Figure 6).

Structural changes of modifier environments following isostatic compression may occur nevertheless, but they are not well understood within this pressure regime. The coordination number of Mg^{2+} has been found to increase with pressure.[53] However, the change in Mg^{2+} coordination number has been observed at much higher pressure than 0.5 GPa. Because MgO is only present in a relatively small amount (<8.5 mol %[25]) in our samples, it seems unlikely that a change in its structural role would cause the observed trend in hardness.

Molecular dynamics simulations[54] have shown that when K^+ is ion exchanged for Na^+, K^+ has an average coordination number between that of Na^+ in the as-quenched sodium glass and that of K^+ in the as-quenched potassium glass. This unique structural setting may be sensitive to structural modifications during precompression, leading to significant changes in the characteristics of the subsequent ion exchange. Indeed, the ^{23}Na NMR results suggest changes in the modifier environments, with increased Na−O mean length and site symmetry for the sample precompressed at 25 C° and 0.5 GPa (Table 3). The obtained NMR results provide information on the average structure of the whole glass. Because isostatic compression affects the surface and interior of the glass equally, the structural change in the Na environment may affect the structural role of K^+, substituted into the Na^+ site during subsequent ion exchange. A change in the structural setting of K^+ may lead to a less pronounced increase of hardness. Furthermore, in order to obtain the constant value of CS observed for the samples precompressed at temperatures below 600 °C (Table 2), a decrease of the network dilation coefficient is required to balance the expected increase of Young's modulus. Such decrease in network dilation coefficient may, analogous to hardness, be related to changes in modifier environments due to precompression. This may explain why hardness did not increase for any of the samples precompressed at temperatures below 600 °C.

A significant increase in CS is observed for the glasses precompressed at 600 °C, indicating that use of a higher temperature during compression allows for significantly different structural rearrangements compared to the glasses precompressed at lower temperatures. NMR results confirm this reasoning, showing a decrease of the mean Na−O bond length for the sample precompressed at 1 GPa and 600 °C (Figure 7), allowing for a greater CS upon substitution with K. The decrease of the Na−O bond length and changes in network bond angles have previously been suggested as important densification mechanisms in glasses of similar compositions at relatively low pressure (<3 GPa).[11] However, the decrease in Na−O bond length observed here is smaller than that previously found from similar pressurization conditions.[16,32−34] This may be a result of thermal relaxation during the subsequent ion exchange for 10 h at 410 °C, erasing a large amount of the changes due to compression only. A decrease in Na−O bond length would be expected to increase the hardness resulting from subsequent ion exchange, but for the samples precompressed at 600 °C, this may be counteracted by a significant decrease in DOL and incorporated amount of K^+ (Figure 3a). The increase in hardness observed for these samples appears to be primarily a result of bulk structural changes in the short- and intermediate-range structures due to compression because both the post- and precompressed samples from these pressurization conditions exhibit similar hardness values (Figure 5), despite having significantly different potassium profiles (Figure 3a,b).

CONCLUSIONS

We have presented an investigation of the impact of pressurization on the density, hardness, and Na^+−K^+ ion exchange properties of an aluminosilicate glass composition that is ion-exchanged either before or after isostatic compression. Significantly increased compressive surface stress (CS) can be achieved in glasses compressed prior to ion exchange, but at the same time, this treatment inhibits fast alkali diffusivity during subsequent ion exchange. In addition, isostatic compression before ion exchange inhibits the increase of hardness that is typically a result of chemical strengthening (i.e., ion exchange). This could be due to structural modifications of the Na^+ site during precompression, affecting the bonding environments of the K^+ ions incorporated into the surface layer during subsequent ion exchange. Compression of the glass after ion exchange causes a relaxation of the compressive surface stress due to the effect of annealing. Hence, the generated compressive stress due to ion exchange can be relaxed even under an applied pressure of 1 GPa.

ASSOCIATED CONTENT

Supporting Information

Examples of optical FSM fringe patterns for three of the investigated samples; K_2O concentration profiles and corresponding erfc fits for selected samples; ^{27}Al 3QMAS NMR spectrum of precompressed sample; example of deconvolution of ^{27}Al MAS NMR spectrum; ^{23}Na 3QMAS NMR data for selected samples. This material is available free of charge via the Internet at http://pubs.acs.org.

AUTHOR INFORMATION

Corresponding Author

*E-mail: mos@bio.aau.dk.

Notes

The authors declare no competing financial interest.

ACKNOWLEDGMENTS

We thank B. Z. Hanson (Corning Incorporated) for EMPA measurements. M.N.S. and M.M.S. acknowledge financial support from the Danish Council for Independent Research under Sapere Aude: DFF-Starting Grant (1335-00051A). S.J.R. acknowledges financial support from the National Science Center of Poland under grant UMO-2011/03/B/ST3/02352.

REFERENCES

(1) Wang, Y.; Ma, Y. Perspective: Crystal Structure Prediction at High Pressures. *J. Chem. Phys.* **2014**, *140*, 040901.
(2) Bundy, F. P. Direct Conversion of Graphite to Diamond in Static Pressure Apparatus. *J. Chem. Phys.* **1963**, *38*, 631−643.
(3) Chang, K. J.; Dacorogna, M. M.; Cohen, M. L.; Mignot, J. M.; Chouteau, G.; Martinez, G. Superconductivity in High-Pressure Metallic Phases of Si. *Phys. Rev. Lett.* **1985**, *54*, 2375−2378.
(4) Takayama-Muromachi, E. High-Pressure Synthesis of Homologous Series of High Critical Temperature (T_c) Superconductors. *Chem. Mater.* **1998**, *10*, 2686−2698.
(5) Matsuoka, T.; Shimizu, K. Direct Observation of a Pressure-Induced Metal-to-Semiconductor Transition in Lithium. *Nature* **2009**, *458*, 186−189.
(6) Badding, J. V.; Meng, J. F.; Polvani, D. A. Pressure Tuning in the Search for New and Improved Solid State Materials. *Chem. Mater.* **1998**, *10*, 2889−2894.
(7) Ovsyannikov, S. V.; Shchennikov, V. V. High-Pressure Routes in the Thermoelectricity or How One Can Improve a Performance of Thermoelectrics. *Chem. Mater.* **2010**, *22*, 635−647.
(8) Greaves, G. N.; Meneau, F.; Majérus, O.; Jones, D. G.; Taylor, J. Identifying Vibrations that Destabilize Crystals and Characterize the Glassy State. *Science* **2005**, *308*, 1299−1302.
(9) Yarger, J. L.; Smith, K. H.; Nieman, R. A.; Diefenbacher, J.; Wolf, G. H.; Poe, B. T.; McMillan, P. F. Al Coordination Changes in High-Pressure Aluminosilicate Liquids. *Science* **1995**, *270*, 1964−1967.
(10) Bouhadja, M.; Jakse, N.; Pasturel, A. Structural and Dynamic Properties of Calcium Aluminosilicate Melts: A Molecular Dynamics Study. *J. Chem. Phys.* **2013**, *138*, 224510.
(11) Allwardt, J. R.; Stebbins, J. F.; Schmidt, B. C.; Frost, D. J.; Withers, A. C.; Hirschmann, M. M. Aluminum Coordination and the Densification of High-Pressure Aluminosilicate Glasses. *Am. Mineral.* **2005**, *90*, 1218−1222.
(12) Grimsditch, M.; Polian, A.; Wright, A. C. Irreversible Structural Changes in Vitreous B_2O_3 Under Pressure. *Phys. Rev. B* **1996**, *54*, 152−155.
(13) Champagnon, B.; Martinet, C.; Boudeulle, M.; Vouagner, D.; Coussa, C.; Deschamps, T.; Grosvalet, L. High Pressure Elastic and Plastic Deformations of Silica: In Situ Diamond Anvil Cell Raman Experiments. *J. Non-Cryst. Solids* **2008**, *354*, 569−573.
(14) McMillan, P. F. New Materials from High-Pressure Experiments. *Nat. Mater.* **2002**, *1*, 19−25.
(15) Wondraczek, L.; Krolikowski, S.; Behrens, H. Kinetics of Pressure Relaxation in a Compressed Alkali Borosilicate Glass. *J. Non-Cryst. Solids* **2010**, *356*, 1859−1862.
(16) Wu, J.; Deubener, J.; Stebbins, J. F.; Grygarova, L.; Behrens, H.; Wondraczek, L.; Yue, Y. Structural Response of a Highly Viscous Aluminoborosilicate Melt to Isotropic and Anisotropic Compressions. *J. Chem. Phys.* **2009**, *131*, 224510.
(17) Striepe, S.; Smedskjaer, M. M.; Deubener, J.; Bauer, U.; Behrens, H.; Potuzak, M.; Youngman, R. E.; Mauro, J. C.; Yue, Y. Elastic and Micromechanical Properties of Isostatically Compressed Soda−Lime−Borate Glasses. *J. Non-Cryst. Solids* **2013**, *364*, 44−52.
(18) Sonneville, C.; De Ligny, D.; Mermet, A.; Champagnon, B.; Martinet, C.; Henderson, G. H.; Deschamps, T.; Margueritat, J.; Barthel, E. In Situ Brillouin Study of Sodium Alumino Silicate Glasses Under Pressure. *J. Chem. Phys.* **2013**, *139*, 074501.
(19) Deschamps, T.; Martinet, C.; de Ligny, D.; Champagnon, B. Elastic Anomalous Behavior of Silica Glass Under High-Pressure: In-Situ Raman Study. *J. Non-Cryst. Solids* **2009**, *355*, 1095−1098.
(20) Käfer, D.; He, M.; Li, J.; Pambianchi, M. S.; Feng, J.; Mauro, J. C.; Bao, Z. Ultra-Smooth and Ultra-Strong Ion-Exchanged Glass as Substrates for Organic Electronics. *Adv. Funct. Mater.* **2013**, *23*, 3233−3238.
(21) Mauro, J. C.; Ellison, A. J.; Pye, L. D. Glass: The Nanotechnology Connection. *Int. J. Appl. Glass Sci.* **2013**, *4*, 64−75.
(22) Wondraczek, L.; Mauro, J. C.; Eckert, J.; Kühn, U.; Horbach, J.; Deubener, J.; Rouxel, T. Towards Ultrastrong Glasses. *Adv. Mater.* **2011**, *23*, 4578−4586.
(23) Varshneya, A. K. Chemical Strengthening of Glass: Lessons Learned and Yet to be Learned. *Int. J. Appl. Glass Sci.* **2010**, *1*, 131−142.
(24) Smedskjaer, M. M.; Mauro, J. C.; Sen, S.; Yue, Y. Quantitative Design of Glassy Materials using Temperature-Dependent Constraint Theory. *Chem. Mater.* **2010**, *22*, 5358−5365.
(25) Dejneka, M. J.; Ellison, A. J.; Mauro, J. C. Ion Exchangable Glass with High Compressive Stress. U.S. Patent 20,130,004,758, Jan 3, 2013.
(26) Guo, X.; Pivovarov, A. L.; Smedskjaer, M. M.; Potuzak, M.; Mauro, J. C. Non-Conservation of the Total Alkali Concentration in Ion-Exchanged Glass. *J. Non-Cryst. Solids* **2014**, *387*, 71−75.
(27) Massiot, D.; Fayon, F.; Capron, M.; King, I.; Le Calvé, S.; Alonso, B.; Durand, J.; Bujoli, B.; Gan, Z.; Hoatson, G. Modelling One- and Two-Dimensional Solid-State NMR Spectra. *Magn. Reson. Chem.* **2002**, *40*, 70−76.
(28) Amoureux, J.; Fernandez, C.; Steuernagel, S. ZFiltering in MQMAS NMR. *J. Magn. Reson., Ser. A* **1996**, *123*, 116−118.
(29) Wu, X.; Moskowitz, J. D.; Mauro, J. C.; Potuzak, M.; Zheng, Q.; Dieckmann, R. Sodium Tracer Diffusion in Sodium Boroaluminosilicate Glasses. *J. Non-Cryst. Solids* **2012**, *358*, 1430−1437.
(30) Risbud, S. H.; Kirkpatrick, R. J.; Taglialavore, A. P.; Montez, B. Solid-State NMR Evidence of 4-, 5-, and 6-Fold Aluminum Sites in Roller-Quenched SiO_2-Al_2O_3 Glasses. *J. Am. Ceram. Soc.* **1987**, *70*, C-10−C-12.
(31) Xue, X.; Stebbins, J. F.; Kanzaki, M.; McMillan, P. F.; Poe, B. Pressure-Induced Silicon Coordination and Tetrahedral Structural Changes in Alkali Oxide-Silica Melts Up to 12 GPa: NMR, Raman, and Infrared Spectroscopy. *Am. Mineral.* **1991**, *76*, 8−26.
(32) Kelsey, K. E.; Stebbins, J. F.; Singer, D. M.; Brown, G. E., Jr.; Mosenfelder, J. L.; Asimow, P. D. Cation Field Strength Effects on High Pressure Aluminosilicate Glass Structure: Multinuclear NMR and La XAFS Results. *Geochim. Cosmochim. Acta* **2009**, *73*, 3914−3933.
(33) Lee, S. K.; Cody, G. D.; Fei, Y.; Mysen, B. O. The Effect of Na/Si on the Structure of Sodium Silicate and Aluminosilicate Glasses Quenched from Melts at High Pressure: A Multi-Nuclear (Al-27, Na-23, O-17) 1D and 2D Solid-State NMR Study. *Chem. Geol.* **2006**, *229*, 162−172.
(34) Lee, S. K. Effect of Pressure on Structure of Oxide Glasses at High Pressure: Insights from Solid-State NMR of Quadrupolar Nuclides. *Solid State Nucl. Magn. Reson.* **2010**, *38*, 45−57.
(35) Lee, S. K.; Yi, Y. S.; Cody, G. D.; Mibe, K.; Fei, Y.; Mysen, B. O. Effect of Network Polymerization on the Pressure-Induced Structural Changes in Sodium Aluminosilicate Glasses and Melts: ^{27}Al and ^{17}O Solid-State NMR Study. *J. Phys. Chem. C* **2012**, *116*, 2183−2191.
(36) Lee, S. K.; Stebbins, J. F. The Distribution of Sodium Ions in Aluminosilicate Glasses: A High-Field Na-23 MAS and 3Q MAS NMR Study. *Geochim. Cosmochim. Acta* **2003**, *67*, 1699−1709.
(37) Xue, X.; Stebbins, J. ^{23}Na NMR Chemical Shifts and Local Na Coordination Environments in Silicate Crystals, Melts, and Glasses. *Phys. Chem. Miner.* **1993**, *20*, 297−307.
(38) George, A. M.; Stebbins, J. F. Dynamics of Na in Sodium Aluminosilicate Glasses and Liquids. *Phys. Chem. Miner.* **1996**, *23*, 526−534.
(39) Stebbins, J. F. Cation Sites in Mixed-Alkali Oxide Glasses: Correlations of NMR Chemical Shift Data with Site Size and Bond Distance. *Solid State Ionics* **1998**, *112*, 137−141.
(40) Angeli, F.; Charpentier, T.; Faucon, P.; Petit, J. Structural Characterization of Glass from the Inversion of Na-23 and Al-27 3Q-MAS NMR Spectra. *J. Phys. Chem. B* **1999**, *103*, 10356−10364.
(41) Charles, R. J. Structural State and Diffusion in a Silicate Glass. *J. Am. Ceram. Soc.* **1962**, *45*, 105−113.
(42) Kroeker, S.; Stebbins, J. F. Magnesium Coordination Environments in Glasses and Minerals: New Insight from High-Field Magnesium-25 MAS NMR. *Am. Mineral.* **2000**, *85*, 1459−1464.
(43) Shimoda, K.; Nemoto, T.; Saito, K. Local Structure of Magnesium in Silicate Glasses: A ^{25}Mg 3QMAS NMR Study. *J. Phys. Chem. B* **2008**, *112*, 6747−6752.

(44) Sen, S.; Maekawa, H.; Papatheodorou, G. N. Short-Range Structure of Invert Glasses Along the Pseudo-Binary Join $MgSiO_3$-Mg_2SiO_4: Results from ^{29}Si and ^{25}Mg MAS NMR Spectroscopy. *J. Phys. Chem. B* **2009**, *113*, 15243−15248.
(45) Scamehorn, C. A.; Angell, C. A. Viscosity−Temperature Relations and Structure in Fully Polymerized Aluminosilicate Melts from Ion Dynamics Simulations. *Geochim. Cosmochim. Acta* **1991**, *55*, 721−730.
(46) Kuryaeva, R. G.; Surkov, N. V. Behavior of the Refractive Index and Compressibility of Albite Glass at Pressures Up to 6.0 GPa. *Geochem. Int.* **2010**, *48*, 835−841.
(47) Kuryaeva, R. G. Effect of High Pressure on the Refractive Index and Density of Natural Aluminosilicate Glasses of Alkali Basalt Composition in the SiO_2-Al_2O_3-TiO_2-Fe_2O_3-P_2O_5-FeO-MnO-CaO-MgO-Na_2O-K_2O System. *Glass Phys. Chem.* **2004**, *30*, 523−531.
(48) Kuryaeva, R. G. Compressibility of Magnesium Silicate Glasses in Comparison with those of Aluminosilicate Glasses. *Solid State Sci.* **2013**, *24*, 133−139.
(49) Deschamps, T.; Martinet, C.; Neuville, D. R.; de Ligny, D.; Coussa-Simon, C.; Champagnon, B. Silica Under Hydrostatic Pressure: A Non Continuous Medium Behavior. *J. Non-Cryst. Solids* **2009**, *355*, 2422−2424.
(50) Seifert, F.; Mysen, B. O.; Virgo, D. Three-Dimensional Network Structure of Quenched Melts (Glass) in the Systems SiO_2-$NaAlO_2$, SiO_2-$CaAl_2O_4$, and SiO_2-$MgAl_2O_4$. *Am. Mineral.* **1982**, *67*, 696−717.
(51) Kuryaeva, R. G.; Surkov, N. V. Behavior of the Refractive Index and Compressibility of Albite Glass at Pressures Up to 6.0 GPa. *Geochem. Int.* **2010**, *48*, 835−841.
(52) Yarger, J. L.; Smith, K. H.; Nieman, R. A.; Diefenbacher, J.; Wolf, G. H.; Poe, B. T.; McMillan, P. F. Al Coordination Changes in High-Pressure Aluminosilicate Liquids. *Science* **1995**, *270*, 1964−1967.
(53) Wilding, M.; Malcolm, G.; Kohara, S.; Bull, C. L.; Akola, J.; Tucker, M. G. The Structure of MgO−SiO_2 Glasses at Elevated Pressure. *J. Phys.: Condens. Matter* **2012**, *24*, 225403.
(54) Tandia, A.; Vargheese, K. D.; Mauro, J. C. Elasticity of Ion Stuffing in Chemically Strengthened Glass. *J. Non-Cryst. Solids* **2012**, *358*, 1569−1574.